

Benzil-Tethered Precipitons for Controlling Solubility: A Round-Trip Energy-Transfer Mechanism in the Isomerization of Extended Stilbene Analogues

Mark R. Ams and Craig S. Wilcox*

Contribution from the Department of Chemistry and The Combinatorial Chemistry Center, University of Pittsburgh, Pittsburgh, Pennsylvania 15260

Received November 16, 2006; E-mail: daylite@pitt.edu

Abstract: We are investigating photoresponsive molecules called “precipitons” that undergo a solubility change co-incident with isomerization. Isomerization can be induced by light or by catalytic reagents. Previous work demonstrated that covalent attachment of a metal complex, Ru(II)(bpy)₃, greatly accelerates photoisomerization and influences the photostationary state. In this paper, we describe precipitons (1,2-biphenylethenes; analogous to stilbenes) that are activated by a covalently attached organic sensitizer (benzil). We find that isomerization of these stilbene analogues is little effected by the presence of benzil in solution but that the intramolecular benzil effect is to increase the rate of isomerization and to significantly change the photostationary state. What is most interesting about these observations is that the precipiton is the primary chromophore in this bichromophoric system (precipiton absorbance is many times greater than benzil absorbance in the 300–400 nm range), yet the neighboring benzil has a significant effect on the rate and the photostationary state. The effect of unattached benzil on the rate was small, about a 24% increase in rate as compared with 4–6-fold changes for an attached benzil. We speculate that the isomerization process occurs by a “round-trip” energy-transfer mechanism. Initial excitation of the precipiton chromophore initiates a sequence that includes (1) formation of the precipiton singlet state, (2) singlet excitation transfer from the precipiton unit to the benzil, (3) benzil-centered intersystem crossing to the localized benzil triplet state, (4) triplet energy transfer from the benzil moiety back to the precipiton, and (5) isomerization.

Introduction

We are interested in crystallization and dissolution and have been investigating stilbene-like molecules that, upon isomerization, exhibit large changes in solubility or phase affinity. Molecules with this property can be used as labels or tags for starting materials or reagents and can be used for removal of unwanted reaction byproducts or metal ions.¹ We call such tags precipitons because isomerization can cause precipitation. Derivatives of **1** undergo photoisomerization, and the isomers have large differences in solubility (Figure 1). Isomer **1Z** is readily soluble in most organic solvents, while the trans form, **1E**, is very insoluble. The solubilities of such isomers (measured as saturated concentrations) can differ by factors greater than 2000.^{1a} The melting points of the trans isomers are greater than 300 °C, while the corresponding cis isomers melt at less than 200 °C. This suggests that the difference in solubility may be caused by enhanced intermolecular contacts (and the corre-

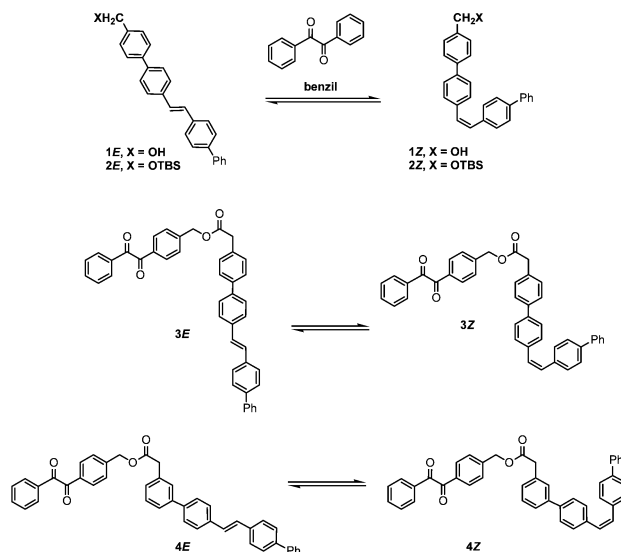
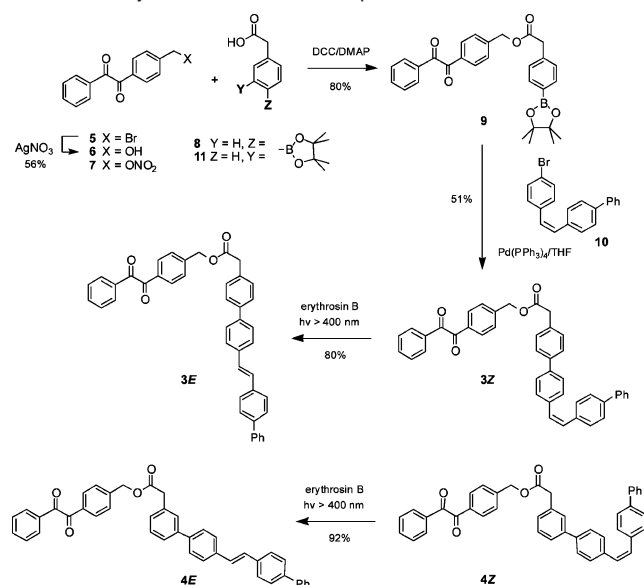


Figure 1. Molecules and equilibria of interest in this study.

sponding increased enthalpy of fusion) in the solid form of the trans isomer compared to that of the cis isomer.

Stilbene isomerization has been studied in great detail for many years.² In recent work, we investigated the effect of a covalently attached photosensitizer, Ru(II)(bpy)₃, on stilbene-

(1) (a) Bosanac, T.; Yang, J.; Wilcox, C. S. *Angew. Chem., Int. Ed.* **2001**, *40*, 1875. (b) Bosanac, T.; Wilcox, C. S. *Chem. Commun.* **2001**, 1618. (c) Bosanac, T.; Wilcox, C. S. *Tetrahedron Lett.* **2001**, *42*, 4309. (d) Bosanac, T.; Wilcox, C. S. *J. Am. Chem. Soc.* **2002**, *124*, 4194. (e) Honigfort, M.; Brittain, W. J.; Bosanac, T.; Wilcox, C. S. *Macromolecules* **2002**, *35*, 4849. (f) Honigfort, M.; Shingta, L.; Rademacher, J.; Malaba, D.; Bosanac, T.; Wilcox, C. S.; Brittain, W. J. ACS Symposium Series 854; American Chemical Society: Washington, DC, 2003; p 250. (g) Bosanac, T.; Wilcox, C. S. *Org. Lett.* **2004**, *6*, 2321.

Scheme 1. Synthesis of Benzil Precipiton Esters

based precipiton isomerization. In the presence of light (>400 nm), the isomerization rate is increased more than 200-fold by the intramolecular Ru(II)(bpy)_3 .³ In this paper, we report our first studies of precipiton isomerization activated by a covalently attached organic sensitizer. The preparation, photophysical properties, and photoisomerization kinetics of precipitons that are covalently linked and unlinked to a benzil⁴ unit are described. The photoisomerization kinetics and photostationary state ratios of the benzil-linked precipitons **3Z/E** and **4Z/E** at a low concentration ($10 \mu\text{M}$) were compared to those of unlinked examples **2Z/E**. Compounds **3Z/E** and **4Z/E** differ in regard to the position of the benzil sensitizer relative to the precipiton (para vs meta). The differences in photoisomerization kinetics and photostationary state ratios will be discussed, and a mechanism for the isomerization will be proposed.

Results and Discussion

Synthesis. The preparation of 1,2-bis(biphenyl)ethene alcohol **1Z**,^{1d} 1,2-bis(biphenyl)ethene TBS ether **2Z/E**,^{1g,3} and precipiton precursor **10**^{1a} have previously been reported from our laboratory. 4-(Bromomethyl)benzil (**5**) is commercially available.

Our original plan was to join the benzil and precipiton moieties through an ether linkage. However, 4-(bromomethyl)-benzil was not stable under base treatment, and attempts at

Table 1. Spectroscopic Data in THF at 298 K

compound	absorption $\lambda_{\text{max}}/\text{nm}$ ($\epsilon/\text{M}^{-1} \text{cm}^{-1}$)	emission $\lambda_{\text{max}}/\text{nm}^a$
2Z	313 (22 610)	387, 409, 432, 465
2E	344 (63 267)	384, 409, 433, 464
benzil	249 (39 103), 255 (43 193), 261 (35 851), 282 (8 303)	413
3Z	249 (12 394), 255 (13 902), 261 (11 862), 319 (25 931)	386, 408, 431
3E	249 (11 761), 255 (12 771), 261 (99 979), 341 (67 480)	386, 408, 431, 464
4Z	249 (59 937), 255 (60 602), 261 (53 967), 306 (23 272)	385, 407, 428, 461
4E	249 (97 959), 255 (109 682), 261 (85 832), 340 (49 315)	385, 407, 432

^a $\lambda_{\text{exc}} = 320$ nm.

coupling 4-(bromomethyl)benzil to precipiton alcohol **1Z** by ether formation using halide abstractor AgO_3SCF_3 resulted in either decomposition (in CH_3NO_2 solvent) or no reaction (in CH_3CN solvent).

We, therefore, pursued coupling based on an ester linkage. Treatment of 4-(bromomethyl)benzil with aqueous AgNO_3 in THF afforded the benzyl alcohol **6** and nitrate ester **7**. Purification by column chromatography on silica gel eluted with 1% EtOAc in CH_2Cl_2 gave alcohol **6** in 56% yield.

For the preparation of conjugate **3Z** (Scheme 1), esterification of alcohol **6** with the para-substituted phenylboronate ester **8** afforded a 94% yield of the benzil-tagged boronic ester **9**. Suzuki coupling between **9** and 1-[2-(4-bromophenyl)]biphenyl ethene **10** afforded the benzil-modified 1,2-bis(biphenyl)ethene analogue **3Z** in 80% yield. Sensitized photoisomerization of **3Z** using erythrosin B in THF afforded trans isomer **3E** in 80% yield.

Synthesis of the meta-linked isomers **4Z** and **4E** followed a similar pathway. Esterification of alcohol **6** with the meta-substituted phenylboronate ester **11** afforded a 59% yield of the benzil-tagged boronic ester **12** (not shown). Suzuki coupling between **12** and 1-[2-(4-bromophenyl)]biphenyl ethene **10** afforded the benzil-modified 1,2-bis(biphenyl)ethene analogue **4Z** in 90% yield. Sensitized photoisomerization of **4Z** using erythrosin B in THF afforded trans isomer **4E** in 92% yield.

Absorption and Emission Spectroscopy. The photophysical data for the compounds are summarized in Table 1. Figure 2 shows the absorption spectra for each compound in neat THF at room temperature. Absorption in the region of 321–377 nm is attributed to the $\pi \rightarrow \pi^*$ transition localized on the ethylene functionality for each precipiton.³ As expected, the ethylene absorption in this region is more intense for the trans isomers compared to that for the cis isomers. The most intense absorptions are seen for the para-substituted precipiton **3E** and the untethered precipiton **2E**. The meta-substituted precipiton **4E** is the weakest absorbing trans isomer. This sequence of absorbance intensity is repeated for the cis isomers.

Benzil exhibits only very weak absorption in the UV range above 300 nm and has insignificant absorption above 340 nm. In our studies of the Ru(II)(bpy)_3 intramolecularly sensitized isomerization of these stilbenes, we used light of wavelengths greater than 400 nm. Our interest here, for practical reasons, was in the behavior of these molecules under the influence of

- (2) (a) Hammond, G. S.; Saltiel, J.; Lamola, A. A.; Turro, N. J.; Bradshaw, J. S.; Cowan, D. D.; Counsell, R. C.; Vogt, V.; Dalton, C. J. *J. Am. Chem. Soc.* **1964**, *86*, 3197. (b) Herkstroeter, W. G.; Hammond, G. S. *J. Am. Chem. Soc.* **1966**, *88*, 4769. (c) Hammond, G. S.; Saltiel, J. *J. Am. Chem. Soc.* **1963**, *85*, 2516. (d) Saltiel, J.; Charlton, J. L.; Mueller, W. B. *J. Am. Chem. Soc.* **1979**, *101*, 1347. (e) Saltiel, J.; Marchand, G. R.; Kirkor-Kaminska, E.; Smothers, W. K.; Mueller, W. B.; Charlton, J. L. *J. Am. Chem. Soc.* **1984**, *106*, 3144. (f) Saltiel, J. S.; Ganapathy, S.; Werking, C. *J. Phys. Chem.* **1987**, *91*, 2755. (g) Waldeck, P. H. *Chem. Rev.* **1991**, *91*, 415. (h) Saltiel, J.; Waller, A. S.; Sears, D. F. *J. Photochem. Photobiol., A* **1992**, *65*, 29. (i) Saltiel, J.; Waller, A. S.; Sears, D. F. *J. Am. Chem. Soc.* **1993**, *115*, 2453.
- (3) Ams, M. R.; Wilcox, C. S. *J. Am. Chem. Soc.* **2006**, *128*, 250.
- (4) (a) Herkstroeter, W. G.; Lamola, A. A.; Hammond, G. S. *J. Am. Chem. Soc.* **1964**, *86*, 4537. (b) Subhas, C. B.; Mukherjee, R.; Chowdhury, M. *J. Chem. Phys.* **1969**, *51*, 754. (c) Wrighton, M. S.; Pdungsap, L.; Morse, D. L. *J. Phys. Chem.* **1975**, *79*, 66. (d) Flamigni, L.; Barigelli, F.; Dellonte, S.; Orlandi, G. *J. Photochem.* **1983**, *21*, 237. (e) Darmann, A. P.; Foote, C. S.; Jardon, P. *J. Phys. Chem.* **1995**, *99*, 11854. (f) Tokunaga, Y.; Akasaka, K.; Hisada, K.; Shimomura, Y.; Kakuchi, S. *Chem. Commun.* **2003**, *17*, 2250. (g) Lopes, S.; Gomez-Zavaglia, A.; Lapinski, L.; Chattopadhyay, N.; Fausto, R. *J. Phys. Chem. A* **2004**, *108*, 8256.

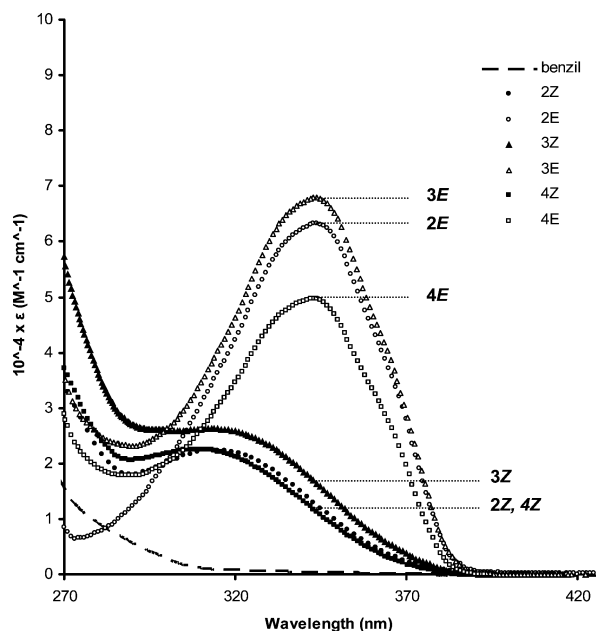


Figure 2. Room-temperature absorption spectra for degassed 10 μM THF solutions of **2Z**, **2E**, **3Z**, **3E**, **4Z**, **4E**, and benzil.

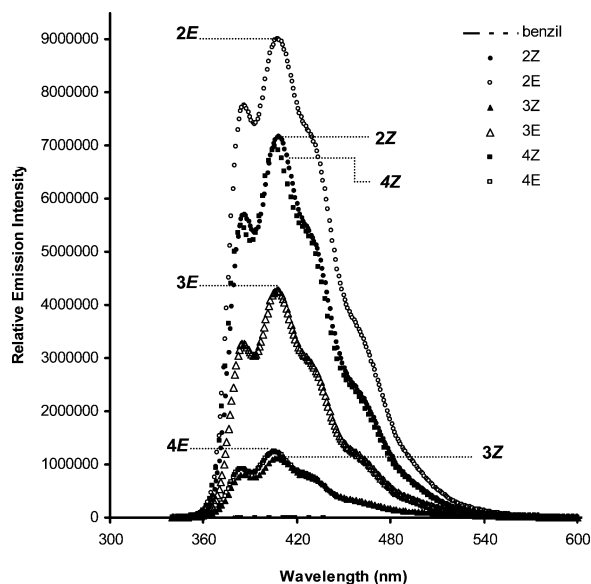


Figure 3. Room-temperature emission spectra for degassed 10 μM THF solutions of **2Z**, **2E**, **3Z**, **3E**, **4Z**, **4E**, and benzil.

inexpensive visible light sources. Therefore, our isomerization studies were conducted with irradiation from an incandescent source without filtering. For the lamp we used, the power output in the 300–320 nm wavelength range is less than 1% of the power output in the 320–400 nm range. We note, before further discussion, that the absorbance of the precipiton moiety is far larger than that of the benzil moiety in the region of highest output from this light source.

Figure 3 illustrates the fluorescence of the investigated compounds upon excitation at 320 nm. Viewing **2E** as the control, these results indicate that the observed precipiton luminescence is quenched when the precipiton is covalently linked to the benzil moiety. The luminescence of **2E** is two times more intense than the luminescence of **3E** and seven times more intense than that of **4E**. The emission positions and vibronic progressions for each precipiton remain unchanged.

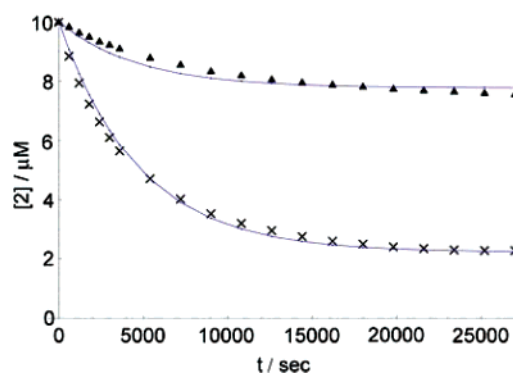


Figure 4. Reaction progress upon irradiation of 10 μM THF solutions of **2Z** (\times) and **2E** (Δ) in the presence of 1 equiv of benzil.

Table 2. Isomerization Rate Constants, Half-Lives, and Photostationary State Ratios for the Photoisomerization Process of **2Z**, **2E**, **3Z**, **3E**, **4Z**, and **4E** upon Irradiation at 10 μM

reaction	$k(\text{s}^{-1}) \times 10^4$	$t_{1/2}(\text{sec})$	Z/E ratio
2Z \rightarrow 2E ^a	1.7	4077	19/81
2E \rightarrow 2Z ^a			
2Z \rightarrow 2E ^b	2.1	3300	22/78
2E \rightarrow 2Z ^b			
3Z \rightarrow 3E	9.5	730	90/10
3E \rightarrow 3Z			
4Z \rightarrow 4E	6.7	1034	76/24
4E \rightarrow 4Z			

^a Reaction observed only for the first half-life. All others were observed for the first five half-lives. ^b Reaction carried out in the presence of benzil (10 μM).

The same quenching effect is observed for **3Z** compared to the untethered **2Z**. The luminescence of **4Z** is interesting in that it is identical with that of **2Z**. The origin of this effect is not clear but is probably not due to the movement of the substituent to the meta position for **4Z**. It has been observed that methyl substitution in different positions on the phenyl rings in *trans*-stilbene has an insignificant effect on absorption and fluorescence spectra.⁵

Photoisomerization Kinetics. To test whether isomerization of the tethered precipiton is influenced by an intramolecular interaction with the nearby benzil chromophore, quantitative rate studies were undertaken. Separate degassed solutions of pure **2Z** and **2E** (10 μM , THF) were irradiated with a 25 W incandescent lamp in the presence of 10 μM benzil sensitizer, and changes in absorbance were monitored at 345 nm. The concentration of **2Z** and **2E** present is plotted as a function of irradiation time in Figure 4. After 7 h of irradiation, solutions containing each pure isomer came to a final Z/E photostationary state, the average ratio of which was determined to be 22/78. The plots analyzed according to a reversible first-order rate curve and the sum of the forward and reverse rate constants for each reaction were averaged and determined to be $k_1 + k_{-1} = 2.1 \times 10^{-4} \text{ s}^{-1}$ (Table 2). There are small deviations from first-order behavior here and with **4E/Z** (Figure 5b) but not in **3Z/E** (Figure 5a). The extent of imperfection correlates with the extent of singlet participation in the process (see discussion below) and is probably caused by minor side reactions from the singlet excited states.

Separate solutions of each isomer **3Z/E** and **4Z/E** were irradiated under the same conditions as those used in the

(5) Samsonova, L. G.; Kopylova, T. N.; Svetlichnaya, N. N.; Andrienko, O. S. *High Energy Chem.* **2002**, 36, 276.

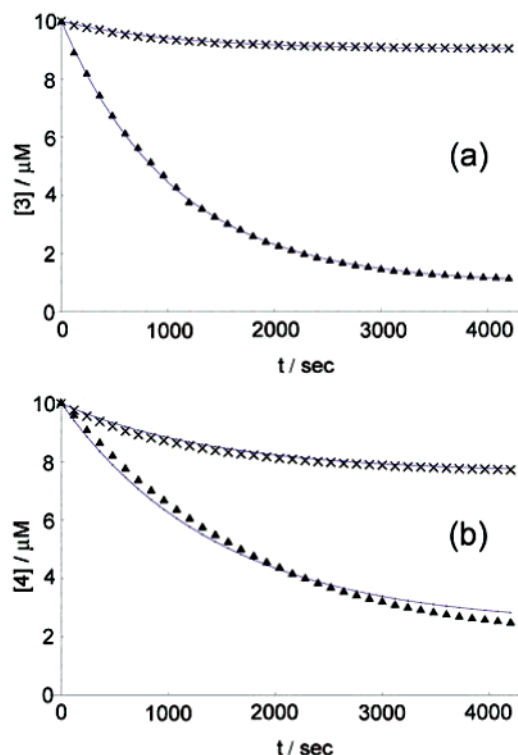


Figure 5. (a) Reaction progress upon irradiation of 10 μM THF solutions of **3Z** (x) and **3E** (▲). (b) Reaction progress upon irradiation of 10 μM THF solutions of **4Z** (x) and **4E** (▲).

isomerization of **2Z/E**. For all isomers, the photostationary state was reached within 70 min. The average ratio of the photostationary state was determined to be 90/10 for **3Z/E** and 76/24 for **4Z/E** (Table 2). The concentration of **E** and **Z** precipiton present is plotted as a function of irradiation time and fits well to a reversible first-order rate curve (Figure 5). The sum of the forward and reverse rate constants for each reaction were averaged and determined to be $k_1 + k_{-1} = 9.5 \times 10^{-4} \text{ s}^{-1}$ for the para-tethered benzil isomers **3Z/E** and $k_1 + k_{-1} = 6.7 \times 10^{-4} \text{ s}^{-1}$ for the meta-tethered benzil isomers **4Z/E**.

A control experiment was performed to evaluate the intermolecular effect of benzil (Table 2). Separate solutions of 10 μM **2Z** and **2E** were prepared in degassed THF and irradiated using the same experimental conditions as those described above. After 7.5 h of irradiation, solutions containing each pure isomer came to a final **Z/E** photostationary state, the average ratio of which was determined to be 19/81. The sum of the forward and reverse rate constants for each reaction were averaged and determined to be $k_1 + k_{-1} = 1.7 \times 10^{-4} \text{ s}^{-1}$.

The effect of covalent attachment of benzil to the precipiton can be observed in the resulting isomerization kinetic data and final photostationary state ratios (Table 2). The first half-life for the direct irradiation of **2Z/E** (no benzil) was weakly effected (1.2 times longer) upon addition of benzil. We conclude that, under these experimental conditions, singlet excitation of the precipiton via direct irradiation plays a major role in the isomerization process⁶ and that benzil contributes only to a minor extent as an intermolecular agent at 10 μM . This is not unexpected upon consideration of the low-light absorption of benzil compared to that of the precipiton in this wavelength range. The final photostationary state ratios were changed only very slightly (toward the cis isomer) by the presence of benzil.

(6) Bortolus, P.; Monti, S. *J. Phys. Chem.* **1979**, *83*, 648.

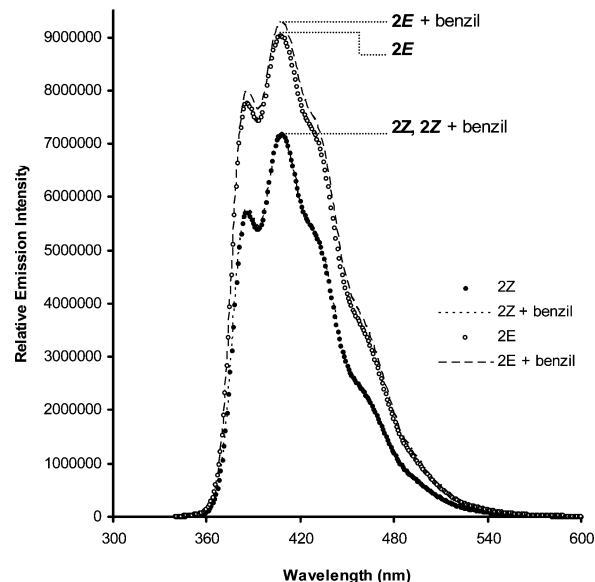


Figure 6. Fluorescence of 10 μM **2Z** and **2E** compared to a solution of **2Z/E** + benzil at the same concentration in THF; $\lambda_{\text{exc}} = 320 \text{ nm}$.

In contrast, when the benzil moiety is covalently attached and thus restricted in distance and orientation relative to the precipiton, the final photostationary states for the isomerizations are significantly shifted in favor of the cis isomers. This effect is most pronounced for the para-substituted benzil-tethered isomers **3Z/E**. Here, the final equilibrium consisted of 90% **Z**-isomer, whereas the intermolecular benzil effect led to only 20% **Z**-isomer. The half-lives for isomerization also decreased significantly for the benzil-tethered precipitons. The first half-life for para-substituted **3Z/E** was completed 4.5 times faster than that for **2Z/E** + benzil, and meta-substituted **4Z/E** was completed 3 times faster than that for **2Z/E** + benzil.

“Round-Trip” Precipiton–Benzil Energy Transfer. An interesting question is posed by these data. How does an attached chromophore (the benzil chromophore), which does not directly absorb light energy, have such a large effect on the photostationary state and also affect the rates of isomerization? We propose that photoisomerization for the precipitons begins with the singlet excited state of the precipiton. The absorbance of this chromophore is dominant within the range of available wavelengths. It is known that isomerization of stilbene upon direct photoexcitation proceeds via a singlet excited state and not a triplet excited state (unless a substituent that promotes intersystem crossing is present).⁷ We expect, therefore, that isomerization of **2Z/E** (Table 2) through direct irradiation also proceeds via a singlet pathway. There was no effect on rate of isomerization of **2Z/E** when an equal concentration of benzil sensitizer was added. This is good evidence against any intermolecular triplet sensitization in the isomerizations of **3Z/E** and **4Z/E**.

Does benzil, at these concentrations, effectively quench the singlet excited state of the precipiton? To test this possibility, fluorescence spectra of **2Z/E** were compared to those of **2Z/E** + benzil (Figure 6). The fluorescence intensity from the precipitons was essentially unchanged when benzil was present, signifying that intermolecular quenching is not occurring at these concentrations (10 μM).

(7) Schuster, D. I.; Nuber, B.; Vail, S. A.; MacMahon, S.; Lin, C.; Wilson, S. R.; Khong, A. *Photochem. Photobiol. Sci.* **2003**, *2*, 315.

Isomerization kinetics are significantly faster for the benzil-tethered precipitons **3Z/E** and **4Z/E**. Why? As shown in Figure 3, the normal stilbene-derived fluorescence caused by singlet excitation for **2E** and **2Z** is considerably quenched for **3Z/E** and **4E**. We propose that this singlet–singlet energy transfer to the benzil moiety is then followed by efficient intersystem crossing to the triplet state of benzil. Benzil has a very low singlet emission quantum yield (~ 0) and a very high intersystem crossing quantum yield (0.9).⁸ Our proposed pathway is consistent with studies in the Rothe labs, wherein they describe benzil acting as an effective “singlet–triplet converter” for polyfluorene sensitization.⁸ Bergamini et al. recently reported a similar forward and backward energy transfer in a dendrimer with peripheral naphthalene units and a benzophenone core.⁹ Ketonic steroids have also been shown to serve as singlet–triplet switches for intramolecular olefin sensitization, although not through a round-trip pathway.¹⁰

Following singlet energy transfer to benzil and intersystem crossing, back-transfer of excitation energy to the precipiton will yield the precipiton triplet excited state. The isomerization rate enhancement for the tethered precipitons over their intermolecularly sensitized unbound analogues is consistent with this triplet energy transfer back to the precipiton, which allows the precipiton to enter upon the triplet energy surface and partake of the usual triplet isomerization pathway.^{2a} Benzil fluorescence overlaps only to a minor extent with precipiton absorption. Therefore, FRET is not likely to contribute significantly to the operative mechanism, and a Dexter-type pathway is more likely.¹¹

A summary of the proposed precipiton–benzil round-trip energy transfer is presented in Figure 7. The approximate energies of the relevant excited levels are based on stilbene and benzil photophysical data. Radiationless transitions are represented by wavy arrows. Our proposal is that excitation of the precipiton affords a singlet excited state localized on the precipiton and that this excitation energy is transferred to the benzil. (The evidence for this lies in the fluorescence quenching observed in the benzil-tethered precipiton isomers.) Rapid ISC affords the benzil-localized triplet, and back-transfer to the precipiton results in the precipiton triplet state and allows efficient isomerization.

The observed photostationary state difference among **2Z/E**, **3Z/E**, and **4Z/E** can best be explained as arising from a competition between direct singlet-state isomerization (in which benzil plays no part) and the round-trip pathway. Introduction of benzil into the solution of **2Z/E** induces a small change in rate and a small change in the photostationary state toward the cis isomer. The propinquity of the benzil chromophore in **3Z/E** and **4Z/E** increases the efficiency of singlet energy transfer to the benzil chromophore, and through back-transfer, increases the effect of the triplet energy pathway of isomerization. The round-trip pathway competes most effectively with the direct pathway in the case of **3Z/E**, where both isomers, upon

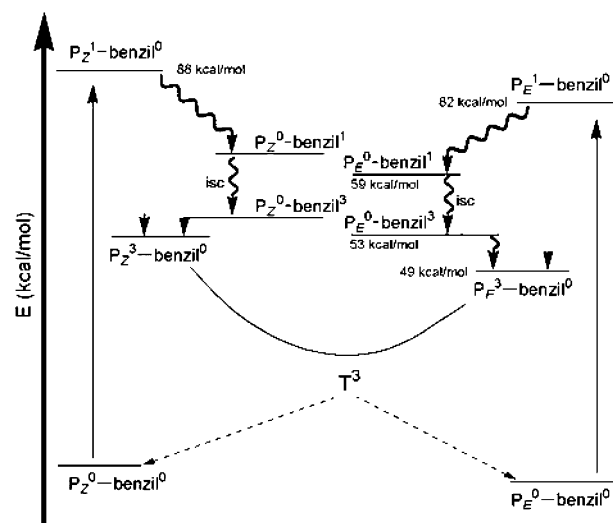


Figure 7. Energy diagram illustrating the “round-trip” precipiton/benzil energy-transfer pathway. P_E^0 -benzil⁰ and P_Z^0 -benzil⁰ represent the ground states of the precipiton–benzil bichromophore. Changes in superscripts identify changes in localized electronic excited states (1 = singlet, 3 = triplet). T3 represents the minimum-energy conformer of the precipiton triplet.

excitation, lead to the formation of the benzil triplet state. In the case of **4Z/E**, only one isomer (**4E**) is quenched by the tethered benzil. The failure of **4Z** to carry singlet energy to the benzil chromophore results in a reduced rate of precipiton triplet-state formation, and the photostationary state is more influenced by the direct singlet pathway.

Conclusions

Our goal was to identify a precipiton derivative that would efficiently isomerize the insoluble trans form of our precipitons to the soluble cis form. Benzil-modified precipiton **4E/Z** meets this need. The molecule will be applied in further investigations of the mechanism of solubilization–isomerization and solubility-based photoswitchable materials.

The round-trip energy-transfer pathway that we discuss here is speculative. The experiments we carried out do not establish this as the only acceptable explanation of the observed results. More sophisticated time-dependent studies will be required to support or refute this proposal. The basic scheme for round-trip energy transfer was proposed by Hammond in 1965 to explain enhanced naphthalene phosphorescence in a benzophenone–naphthalene bichromophoric system.¹² In that case, in the Rothe work with benzil,⁸ and in the recent work by Bergamini et al. with benzophenone,⁹ the round trip concluded with enhanced triplet-state emission from a readily excited chromophore that was inefficient in intersystem crossing. In those studies as in ours, the enhancement occurred due to the effect of a nearby partner. In those studies, the evidence for the round trip was based on total emission measurements. To our knowledge, the work described here provides the first example of a round trip leading to a chemical event; here, it is the chemical event that provides the evidence of the round trip. It may interest the reader to note that the benzil effect is geometrically selective. The round-trip mechanism opens access

- (8) Rothe, C.; Palsson, L. O.; Monkman, A. P. *Chem. Phys.* **2002**, 285, 95.
- (9) Bergamini, G.; Ceroni, P.; Maestri, M.; Balzani, V.; Lee, S. K.; Vogtle, F. *Photochem. Photobiol. Sci.* **2004**, 3, 898.
- (10) Agyin, J. K.; Timberlake, L. D.; Morrison, H. J. *Am. Chem. Soc.* **1997**, 119, 7945.
- (11) (a) Förster, Th. H. *Discuss. Faraday Soc.* **1959**, 27, 7. (b) Dexter, D. L. *J. Chem. Phys.* **1953**, 21, 836. (c) Mondal, J. A.; Ramakrishna, G.; Singh, A. K.; Ghosh, H. N.; Mariappan, M.; Maiya, B. G.; Mukherjee, T.; Palit, D. K. *J. Phys. Chem. A* **2004**, 108, 7843.

- (12) Lamola, A. A.; Leermakers, P. A.; Byers, G. W.; Hammond, G. S. *J. Am. Chem. Soc.* **1965**, 87, 2322.

to the precipiton triplet state but does so to different extents for the *Z* and *E* isomers and for the meta- and para-linked chromophores. This is surely because the geometry of the molecules and their conformational microstates influence the efficiency of intramolecular singlet energy transfer and also affect the back-transfer of triplet excitation energy. Which effect is most important, if either, is unknown. We believe it may be productive to contemplate potential uses of this stereoselectivity in energy transfer for any investigator interested in new separation strategies and new chemoselective processes.

Experimental Section

Introduction. The compound 4-(bromomethyl)benzil (**5**) and the boronic acid pinacol esters **8** and **11** were commercially available and were used as received. Preparation and purification of the tethered precipitons **3Z/E** and **4Z/E** were carried out in a darkened laboratory under red-light illumination.

4-(Hydroxymethyl)benzil (6) and 4-(Hydroxymethyl)benzil Nitrate (7). To a solution of 4-(bromomethyl)benzil (**5**, 100 mg, 0.33 mmol) in 33 mL of THF was added a solution of AgNO₃ (653 mg, 0.38 mmol) in 11 mL of water. The resulting mixture was heated at reflux for 3.5 h. After the mixture was cooled, precipitated AgBr was removed by filtration and rinsed with acetone. Volatile components of the filtrate were removed in vacuo, and the resulting mixture was extracted with CH₂Cl₂ (3 × 50 mL). The CH₂Cl₂ extracts were combined, washed with brine (150 mL), dried with MgSO₄, and filtered. Volatile components of the filtrate were removed in vacuo, and purification of the residue by flash chromatography (SiO₂, 1% EtOAc in CH₂Cl₂) afforded, first, 4-(hydroxymethyl)benzil nitrate **7** as a yellow oil (42.8 mg): *R*_f 0.79 (1% EtOAc in CH₂Cl₂); IR (thin film) 2924, 1672, 1626, 1607, 1596, 1580, 1450, 1279, 1211, 1173 cm⁻¹; ¹H NMR (300 MHz, CDCl₃) δ 8.04–7.97 (m, 4H), 7.69 (dddd, *J* = 8, 8, 1, 1 Hz, 1H), 7.54 (app d, *J* = 6 Hz, 3H), 7.51 (m, 1H), 5.50 (s, 1H); ¹³C NMR (75 MHz, CH₂Cl₂) δ 194.0, 193.6, 139.4, 135.0, 133.6, 132.8, 130.3, 129.9, 129.1, 128.8, 73.3; HRMS (EI) *m/e* calcd for C₁₅H₁₁NO₃, 285.063723; found; 285.063638. Further elution (SiO₂, 1% EtOAc in CH₂Cl₂) afforded alcohol **6** as a light-yellow wax (25.9 mg, 56%): *R*_f 0.21 (2% EtOAc in CH₂Cl₂); IR (thin film) 3419, 3062, 2923, 1674, 1605, 1579 cm⁻¹; ¹H NMR (300 MHz, CDCl₃) δ 7.98 (app d, *J* = 8 Hz, 4H), 7.68 (dddd, *J* = 8, 8, 2, 2 Hz, 1H), 7.53 (m, 4H), 4.82 (s, 2H); ¹³C NMR (75 MHz, CH₂Cl₂) δ 194.6, 194.2, 148.4, 134.9, 133.0, 132.2, 130.3, 129.9, 129.0, 126.9, 64.4; HRMS (EI) *m/e* calcd for C₁₅H₁₂O₃, 240.0786; found, 240.0776.

[4-(2-Oxo-2-phenylacetyl)phenyl]acetic Acid 4-(4,4,5,5-Tetramethyl-[1,3,2]dioxaborolan-2-yl)benzyl Ester (9). To stirred a solution of 4-(hydroxymethyl)benzil **6** (968 mg, 4.03 mmol) and para-substituted carboxylic acid pinacol ester **8** (1.05 g, 3.99 mmol) in anhydrous CH₂Cl₂ (40 mL), at 0 °C, were added 4-(dimethylamino)pyridine (DMAP, 97.4 mg, 0.798 mmol) and dicyclohexylcarbodiimide (DCC, 905 mg, 4.39 mmol). The solution was stirred for 10 min at 0 °C and then warmed to room temperature and stirred for 3 h. The white precipitate that formed was removed by filtration, and the volatile components of the filtrate were removed in vacuo to give a yellow oil that was purified by flash chromatography (SiO₂, 1% EtOAc in CH₂Cl₂) to afford **9** as a yellow oil (1.81 g, 94%): *R*_f 0.55 (CH₂Cl₂); IR (thin film) 3399, 2978, 1736, 1678, 1608, 1450, 1360, 1322, 1274, 1213, 1174, 1143 cm⁻¹; ¹H NMR (300 MHz, CDCl₃) δ 7.99–7.94 (m, 4H), 7.78 (d, *J* = 8 Hz, 2H), 7.68 (dddd, *J* = 8, 8, 1, 1 Hz, 1H), 7.55–7.50 (m, 2H), 7.42 (d, *J* = 9 Hz, 2H), 7.30 (d, *J* = 8 Hz, 2H), 5.19 (s, 2H), 3.72 (s, 2H), 1.35 (s, 12H); ¹³C NMR (75 MHz, CH₂Cl₂) δ 194.2, 193.9, 170.8, 143.1, 136.6, 135.1, 134.8, 132.9, 132.6, 130.1, 129.9, 129.0, 128.6, 127.9, 83.8, 65.5, 41.5, 24.8; HRMS (ES) *m/e* calcd for C₂₉H₂₉BO₆Na, 507.1955; found, 507.1947.

[4-(2-Oxo-2-phenylacetyl)phenyl]acetic Acid 3-(4,4,5,5-Tetramethyl-[1,3,2]dioxaborolan-2-yl)benzyl Ester (12). To stirred a

solution of 4-(hydroxymethyl)benzil **6** (1.02 g, 4.26 mmol) and meta-substituted carboxylic acid pinacol ester **11** (1.10 g, 4.21 mmol) in anhydrous CH₂Cl₂ (43 mL), at 0 °C, were added 4-(dimethylamino)pyridine (DMAP, 103 mg, 0.843 mmol) and dicyclohexylcarbodiimide (DCC, 957 mg, 4.64 mmol). The solution was stirred for 10 min at 0 °C and then warmed to room temperature and stirred for 2.5 h. The white precipitate that formed was removed by filtration, and the volatile components of the filtrate were removed in vacuo to give a yellow oil that was purified by flash chromatography (SiO₂, 1% EtOAc in CH₂Cl₂) to afford **12** as a yellow oil (1.21 g, 59%): *R*_f 0.61 (1% EtOAc in CH₂Cl₂); IR (thin film) 3057, 2978, 2931, 1740, 1674, 1608, 1430, 1360, 1323, 1213, 1144, 1099, 1000, 709 cm⁻¹; ¹H NMR (300 MHz, CDCl₃) δ 7.95 (app t, *J* = 14, 6 Hz, 4H), 7.74 (m, 2H), 7.64 (app t, *J* = 14, 7, 1 Hz, 1H), 7.50 (app t, *J* = 15, 8 Hz, 2H), 7.43–7.31 (m, 4H), 5.19 (s, 2H), 3.71 (s, 2H), 1.34 (s, 12H); ¹³C NMR (75 MHz, CH₂Cl₂) δ 194.2, 193.8, 170.9, 143.1, 135.1, 134.8, 133.6, 132.8, 132.5, 132.0, 130.0, 129.8, 128.9, 128.0, 127.8, 83.4, 65.3, 41.0, 24.8; HRMS (ES) *m/e* calcd for C₂₉H₂₉BO₆Na, 507.1955; found, 507.197.

[4'-(2-Biphenyl-4-yl-vinyl)biphenyl-4-yl]acetic Acid 4-(2-Oxo-2-phenylacetyl)benzyl Ester (3Z). A solution of 1-[2-(4-bromophenyl)]-biphenyl ethene **10** (555 mg, 1.66 mmol), pinacol boronic ester **9** (884 mg, 1.82 mmol), and Pd(PPh₃)₄ (82.5 mg, 0.071 mmol) in THF (10.3 mL) was degassed via three freeze–pump–thaw cycles and placed under nitrogen. Sodium carbonate (527 mg, 4.97 mmol), which had been dissolved in a minimum amount of water in a separate flask and degassed similarly, was transferred to the THF solution via cannula. The resulting mixture was heated at reflux for 20 h. After the mixture was cooled, volatile components were removed in vacuo, and the crude residue was combined with water (100 mL) and extracted with CH₂Cl₂ (3 × 100 mL). The CH₂Cl₂ extracts were combined, washed with brine (300 mL), dried with MgSO₄, and filtered. Volatile components of the filtrate were removed in vacuo, and the residue was purified by flash chromatography (SiO₂, 7:3 CH₂Cl₂/Hex) to afford **3Z** as a light-yellow wax (81.3 mg, 80%): *R*_f 0.39 (7:3 CH₂Cl₂/Hex); mp 82–84 °C; IR (thin film) 3028, 1738, 1671, 1608, 1596, 1496, 1486, 1449, 1416, 1213, 1173, 1146, 1006, 883 cm⁻¹; ¹H NMR (300 MHz, CDCl₃) δ 7.98–7.94 (m, 4H), 7.71–7.30 (m, 22H), 6.66 (s, 2H), 5.22 (s, 2H), 3.74 (s, 2H); ¹³C NMR (75 MHz, CH₂Cl₂) δ 194.2, 193.9, 171.0, 143.1, 140.6, 139.9, 139.7, 139.3, 136.4, 136.3, 134.9, 133.0, 132.7, 132.6, 130.1, 130.0, 129.9, 129.7, 129.4, 129.3, 129.0, 128.7, 128.0, 127.4, 127.3, 127.1, 127.0, 126.9, 126.85, 126.75; HRMS (EI) *m/e* calcd for C₄₃H₃₂O₄, 612.230060; found, 612.232163.

[4'-(2-Biphenyl-4-yl-vinyl)biphenyl-4-yl]acetic Acid 4-(2-Oxo-2-phenylacetyl)benzyl Ester (3E). A solution of precipiton **3Z** (100 mg, 0.163 mmol) and erythrosine B (6.8 mg, 0.008 mmol) in THF (1.63 mL) was degassed via three freeze–pump–thaw cycles and then placed under nitrogen. The resulting mixture was stirred and irradiated with a 250 W incandescent lamp for 20 h. The resulting precipitate **3E** (70.8 mg, 71%) was isolated by filtering the reaction mixture through filter paper and washing it with THF until all traces of the red dye were removed: mp >240 °C; IR (KBr) 3030, 1729, 1665, 1608, 1496, 1450, 1409, 1374, 1243, 1162, 1003, 971 cm⁻¹; ¹H NMR (300 MHz, CDCl₃) δ 7.99–7.96 (m, 4H), 7.68–7.34 (m, 22H), 7.21 (s, 2H), 5.24 (s, 2H), 3.76 (s, 2H); ¹³C NMR, too insoluble to obtain; HRMS (EI) *m/e* calcd for C₄₃H₃₂O₄, 612.230060; found, 612.232850.

[4'-(2-Biphenyl-4-yl-vinyl)biphenyl-3-yl]acetic Acid 4-(2-Oxo-2-phenylacetyl)benzyl Ester (4Z). A solution of 1-[2-(4-bromophenyl)]-biphenyl ethene **10** (372 mg, 1.11 mmol), pinacol boronic ester **12** (592 mg, 1.22 mmol), and Pd(PPh₃)₄ (55.4 mg, 0.048 mmol) in THF (6.9 mL) was degassed via three freeze–pump–thaw cycles and then placed under nitrogen. Sodium carbonate (353 mg, 3.33 mmol), previously dissolved in a minimum amount of water in a separate flask and degassed similarly, was transferred to the THF solution via cannula. The resulting mixture was heated at reflux for 23 h. After the mixture was cooled, volatile components were removed in vacuo, and the crude residue was combined with water (100 mL) and extracted with CH₂-

Cl₂ (3 × 100 mL). The CH₂Cl₂ extracts were combined, washed with brine (300 mL), dried with MgSO₄, and filtered. Volatile components of the filtrate were removed in vacuo, and the residue was purified by flash chromatography (SiO₂, 8:2 Hex/CH₂Cl₂) to afford **4Z** as a light-yellow wax (608 mg, 90%): *R*_f 0.16 (5:5 Hex/CH₂Cl₂); mp 44–46 °C; IR (thin film) 3056, 3029, 1739, 1672, 1607, 1579, 1485, 1449, 1417, 1241, 1212, 1174, 1147, 883 cm⁻¹; ¹H NMR (300 MHz, CDCl₃) δ 8.03 (app t, 4H), 7.68–7.28 (m, 22H), 6.73 (s, 2H), 5.25 (s, 2H), 3.81 (s, 2H); ¹³C NMR (75 MHz, CH₂Cl₂) δ 194.0, 193.7, 170.7, 142.9, 140.8, 140.3, 139.6, 139.1, 136.3, 136.0, 134.7, 133.9, 132.7, 132.4, 129.9, 129.7, 129.6, 129.2, 128.9, 128.8, 128.5, 128.0, 127.8, 127.6, 127.1, 126.8, 126.6, 125.6, 65.3, 40.1; HRMS (ES) *m/e* calcd for C₄₃H₃₂O₄Na, 635.2218; found, 635.2198.

[4'-(2-Biphenyl-4-yl-vinyl)biphenyl-3-yl]acetic Acid 4-(2-Oxo-2-phenylacetyl)benzyl Ester (4E). A solution of precipiton **4Z** (66.8 mg, 0.109 mmol) and erythrosine B (4.6 mg, 0.006 mmol) in THF (1.09 mL) was degassed via three freeze–pump–thaw cycles and then placed under nitrogen. The resulting mixture was stirred and irradiated with a 250 W incandescent lamp equipped with a λ ≤ 400 nm cutoff filter for 4 h. The resulting homogeneous solution was then purified by flash chromatography (SiO₂, 8:2 Hex/CH₂Cl₂) to afford **4E** as a light-yellow solid (61.4 mg, 92%): mp 181–183 °C; IR (KBr) 3434, 3030, 1736, 1670, 1607, 1596, 1579, 1486, 1449, 1408, 1375, 1213, 1174, 1146, 1004, 970 cm⁻¹; ¹H NMR (300 MHz, CDCl₃) δ 7.99–7.95 (m, 4H), 7.69–7.30 (m, 22H), 7.21 (s, 2H), 5.24 (s, 2H), 3.79 (s, 2H); ¹³C NMR,

too insoluble to obtain; HRMS (EI) *m/e* calcd for C₄₃H₃₂O₄, 612.230060; found, 612.230060.

Photochemical Experiments. All of the photochemical measurements were performed in degassed THF. UV–vis absorption spectra were recorded with a PerkinElmer Lambda 9 UV–vis spectrophotometer. Photoisomerization experiments were monitored by recording the UV–vis absorption of **2Z/E**, **3Z/E**, and **4Z/E** at 345 nm exclusively. All experiments were performed in the dark or under red light due to the high sensitivity of the compounds to normal ambient lighting. Emission spectra were recorded with a 1680/1681 Spex Fluorolog spectrometer. The excitation light used for all of the photoisomerization experiments was produced by a 25 W incandescent lamp positioned 5 cm from the degassed cuvette which contained the sample.

Acknowledgment. Financial support from the National Institute of General Medical Sciences is gratefully acknowledged. The authors would also like to recognize the help of Prof. David Waldeck and Prof. Stephane Petoud.

Supporting Information Available: Experimental details, ¹H and ¹³C NMR spectra, and complete characterization data for all compounds. This material is available free of charge via the Internet at <http://pubs.acs.org>.

JA068211C